

Supporting Information for

**Fine Regulation of the Cellulose Dissolution and Regeneration by
Low Pressure CO₂ in DMSO/Organic Base: the Dissolution Behavior
and Mechanism**

Jinfang Wang,^a Zhimin Xue,^b Chuanyu Yan,^a Zhonghao Li,^c and Tiancheng Mu^{a*}

*Corresponding author. Email: tcmu@ruc.edu.cn

Content:

1. Solubility and thermodynamic parameters of MCC in CO₂-DMSO/organic base solvent system: Figure S1, Tables S1, S2, and S3.
2. Solvatochromic parameters: Table S4 and Figure S2.
3. Error analysis: Tables S5 and S6.
4. Original ATR-FTIR spectrums and instruments photos for measuring ATR-FTIR spectrums: Figures S3 and S4.
5. Original NMR data: Figures S5 and S6.
6. UV-Vis spectrums and instruments photos for measuring UV-Vis spectrums: Figures S7 and S8.
7. Electrostatic potential (ESP) results: Figure S9.
8. Characterization and analysis of the regenerated cellulose: Figure S10.
9. Reusability/recyclability of the solvent system: Figure S11.

1. Solubility and thermodynamic parameters of MCC

The dissolved MCC solution, in which DMSO was replaced by d-DMSO, was syringed to an NMR tube under N_2 environment. Then CO_2 was sparged through the solution for 5 min, the tube was quickly capped and sealed. The CO_2 pressure was 1 atm at 303 K. Equilibrium constant (K_{eq}) was calculated through the concentrations of species plus the pressure of CO_2 .¹

Table S1 Solubility of MCC in CO_2 -DMSO/DBU solvent system at different W_{DBU} (dissolving condition: P_{CO_2} = 1 atm; $T=303$ K; $t=1$ h)

No.	W_{DBU}	Solubility		K_{eq}
		(g/100 g solvent)		
1	0.05	5.7		0.54
2	0.1	9.0		0.42
3	0.2	8.6		0.20
4	0.3	8.1		0.13
5	0.4	7.5		0.09
6	0.5	5.5		0.05

Rationale for the appearance of error bars for the solubility

1. As the water bath can't keep the temperature absolutely uniform, the slightly temperature change may cause the CO_2 pressure change in the high-pressure cell, which further influence the cellulose solubility.
2. While we try to reduce the stirring rate, there might be a very small amount of cellulose attached to the inner wall and can't participate dissolving. It will also affect the solubility.

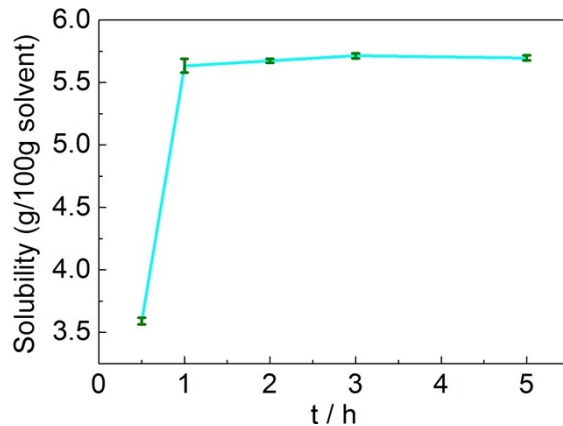


Fig. S1 Effect of dissolving time on the solubility of MCC (dissolving condition: P_{CO_2} =0.1 MPa; $T=303.15$ K; W_{DBU} =0.1).

Table S2 Solubility of MCC in CO₂-DMSO/DBU solvent system at different temperature and pressure

No.	Atmosphere	Solubility (gram per 100 g of the solvent)		
		P / MPa	303K	313K
1	CO ₂	0.1	5.5	5.6
2	CO ₂	0.2	8.6	9.0
3	CO ₂	0.3	8.8	8.9
4	CO ₂	0.5	7.5	7.6
5	CO ₂	0.7	7.0	7.2
6	CO ₂	1.0	6.3	6.4
				6.7

According to the solubility data of MCC, the standard Gibbs energy (ΔG^θ) can be obtained by the following eqn:

$$\Delta G^\theta = -RT\ln K_{eq} \quad (1)$$

$$K_{eq} = \frac{[BaseH^+] [ROCO_2^-]}{P_{CO_2} [Base] [ROH]} \quad (2)$$

Where T stands for temperature; K_{eq} is the equilibrium constant and can be calculated based on the reported method.¹ The standard enthalpy (ΔH^θ) may be obtained by eqn (3) according to the Van't Hoff equation and the standard entropy (ΔS^θ) can be calculated by eqn (4).

$$\frac{d\ln K_{eq}}{dT} = \frac{\Delta H^\theta}{R T^2} \quad (3)$$

$$\Delta G^\theta = \Delta H^\theta - T \Delta S^\theta \quad (4)$$

All thermodynamic parameters calculated are listed in Tables S4. For CO₂-DMSO/DBU solvent system, ΔH^θ values and ΔS^θ values are negative at almost whole temperature range, which indicates that the MCC dissolving process is enthalpy driven. The change of ΔS^θ values from positive to negative with the increase of CO₂ pressure means the dissolving process of MCC is entropy driven at low CO₂ pressure while it is different at high CO₂ pressure. The ΔG^θ values changed from negative to positive with increasing pressure. It means the interaction between MCC and organic base is thermodynamic favorable at low CO₂ pressure and thermodynamic unfavorable at relatively high CO₂ pressure. Moreover, it further suggests that the energy cost increased with the pressure increasing. Therefore, appropriate pressure is important for the dissolution of MCC in DMSO/DBU solvent system.

Table S3 The Thermodynamic Parameters of MCC in the CO₂-DMSO/DBU Solvent System at Different Temperature and Pressure

parameters	T / K	P / MPa					
		0.1	0.2	0.3	0.5	0.7	1.0
	303	-3.89	-1.01	0.07	0.95	1.63	2.28
ΔG ^θ (kJ mol ⁻¹)	313	-1.18	1.87	2.89	3.81	4.55	5.15
	323	-1.03	1.86	2.92	3.86	4.65	5.46
	303	-84.27	-85.43	-82.82	-82.47	-84.11	-82.26
ΔH ^θ (kJ mol ⁻¹)	313	-47.90	-44.66	-43.26	-47.18	-44.30	-46.07
	323	-6.25	1.95	1.97	-6.77	1.22	-4.65
	303	-265.16	-278.47	-273.41	-275.19	-282.81	-278.84
ΔS ^θ (J mol ⁻¹)	313	-149.19	-148.58	-147.38	-162.84	-155.99	-163.58
	323	-16.17	0.28	-2.95	-32.90	-10.64	-31.30

2. Solvatochromic parameters

Table S4 Solvatochromic Parameters in CO₂-DMSO/DBU Solvent System at Different Temperature and Pressure

Temperature	P / MPa	Kamlet – Taft parameters of the solvent system			
		A	β	π	β-α
303 K	0.0	0.81	1.20	0.59	0.39
	0.1	0.85	1.00	0.63	0.15
	0.2	0.87	0.92	0.65	0.05
	0.3	0.78	1.26	0.57	0.48
	0.5	0.85	1.07	0.63	0.22
	0.7	0.84	1.07	0.62	0.23
	1.0	0.74	1.12	0.54	0.37
313 K	0.0	0.80	1.23	0.59	0.43
	0.1	0.84	0.92	0.63	0.08
	0.2	0.83	0.87	0.62	0.04
	0.3	0.72	1.24	0.52	0.52
	0.5	0.75	1.14	0.55	0.39

	0.7	0.73	1.16	0.53	0.43
	1.0	0.73	1.09	0.53	0.36
	0.0	0.66	1.27	0.48	0.60
	0.1	0.75	0.96	0.55	0.21
	0.2	0.73	0.88	0.53	0.16
323 K	0.3	0.72	1.14	0.52	0.42
	0.5	0.73	1.13	0.54	0.40
	0.7	0.72	1.05	0.53	0.32
	1.0	0.71	1.07	0.51	0.36

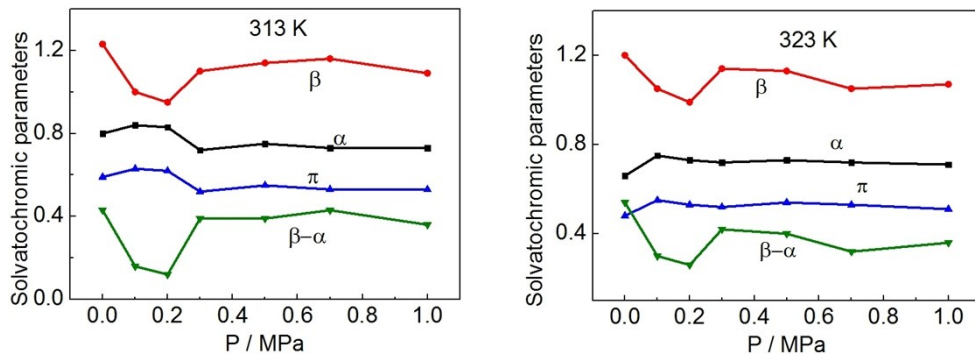


Fig. S2 Solvatochromic parameters in CO₂-DMSO/DBU solvent system at different temperature and pressure: black is α , red is β , blue is π , olive is $\beta-\alpha$.

3. Error analysis

Standard Deviation:

$$S = \sqrt{\frac{1}{N-1} \sum_{i=1}^N (X_i - \bar{X})^2}$$

Table S5 Effect of W_{DBU} on the solubility of MCC (dissolving condition: $P_{CO_2}=0.2$ MPa; $T=323.15$ K; dissolving time: 1h).

W _{DBU} (%)	Solubility (gram per 100 g of the solvent)				Standard Deviation (S)
	1	2	3	Mean	
0.05	5.70	5.50	5.60	5.60	0.10
0.10	9.00	8.80	9.10	8.97	0.15
0.20	8.60	9.00	8.70	8.77	0.21
0.30	8.10	8.00	8.15	8.08	0.08
0.40	7.50	7.30	7.40	7.40	0.10
0.50	5.50	5.40	5.50	5.47	0.06

Table S6 Effect of dissolving time on the solubility of MCC (dissolving condition: $P_{CO_2}=0.1$ MPa; $T=303.15$ K; $W_{DBU}=0.1$).

t (h)	Solubility (gram per 100 g of the solvent)				Standard Deviation (S)
	1	2	3	Mean	
0.5	3.58	3.62	3.57	3.59	0.03
1	5.63	5.69	5.58	5.63	0.06
2	5.67	5.66	5.69	5.67	0.02
3	5.69	5.72	5.75	5.71	0.02
5	5.69	5.68	5.72	5.70	0.02

4. Original ATR-FTIR spectrums and instrument photos



Fig. S3 The photos of instrument for ATR-FTIR measurement

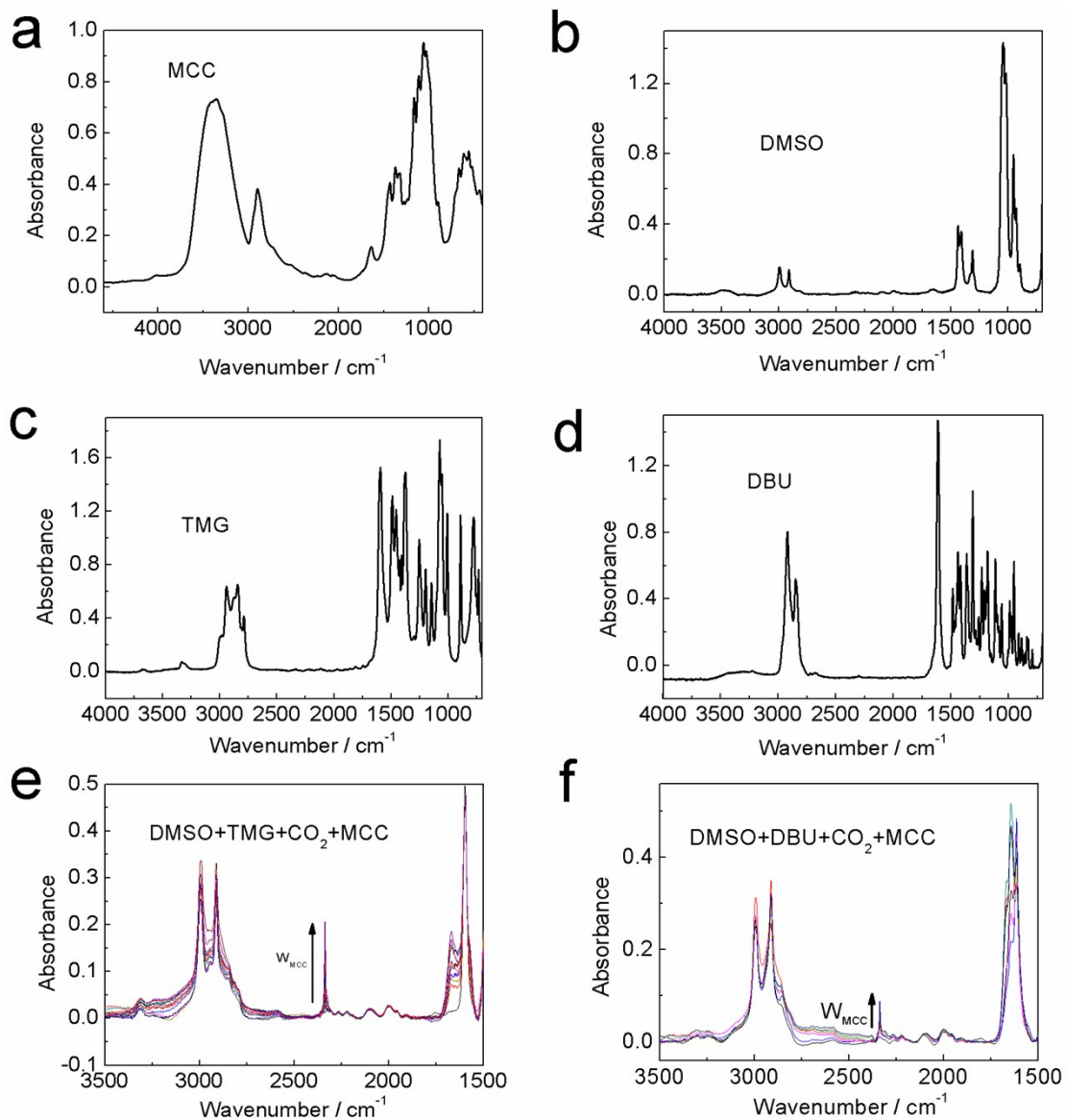
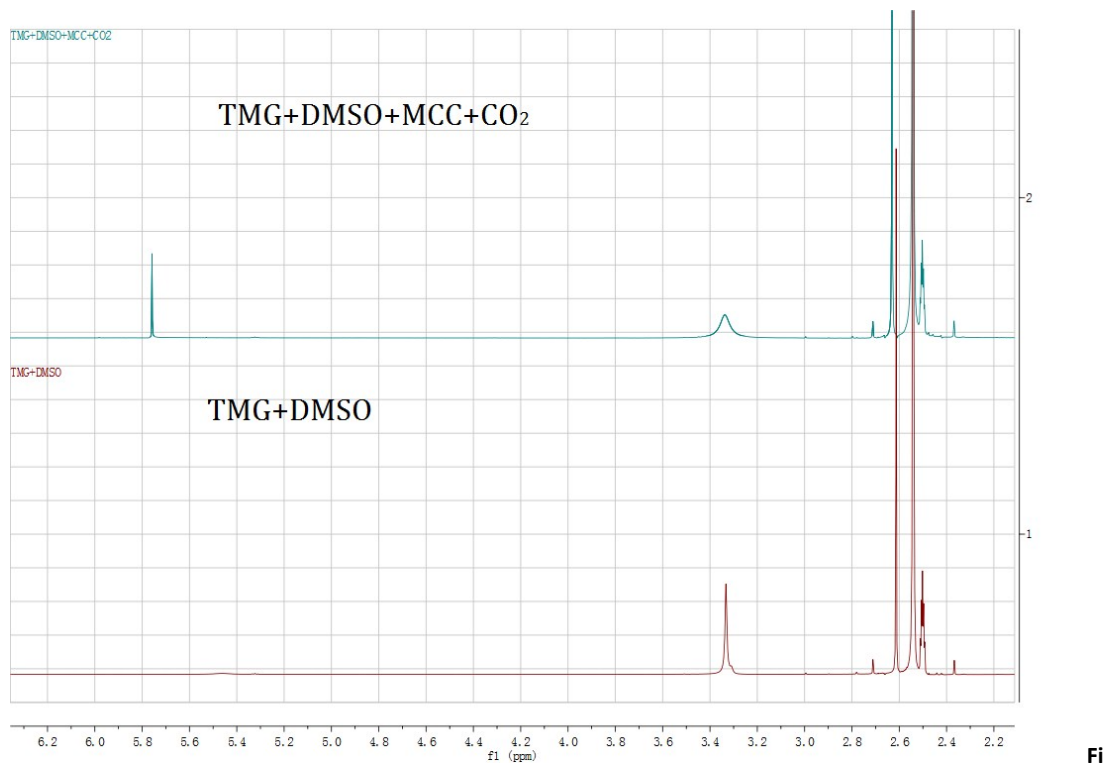
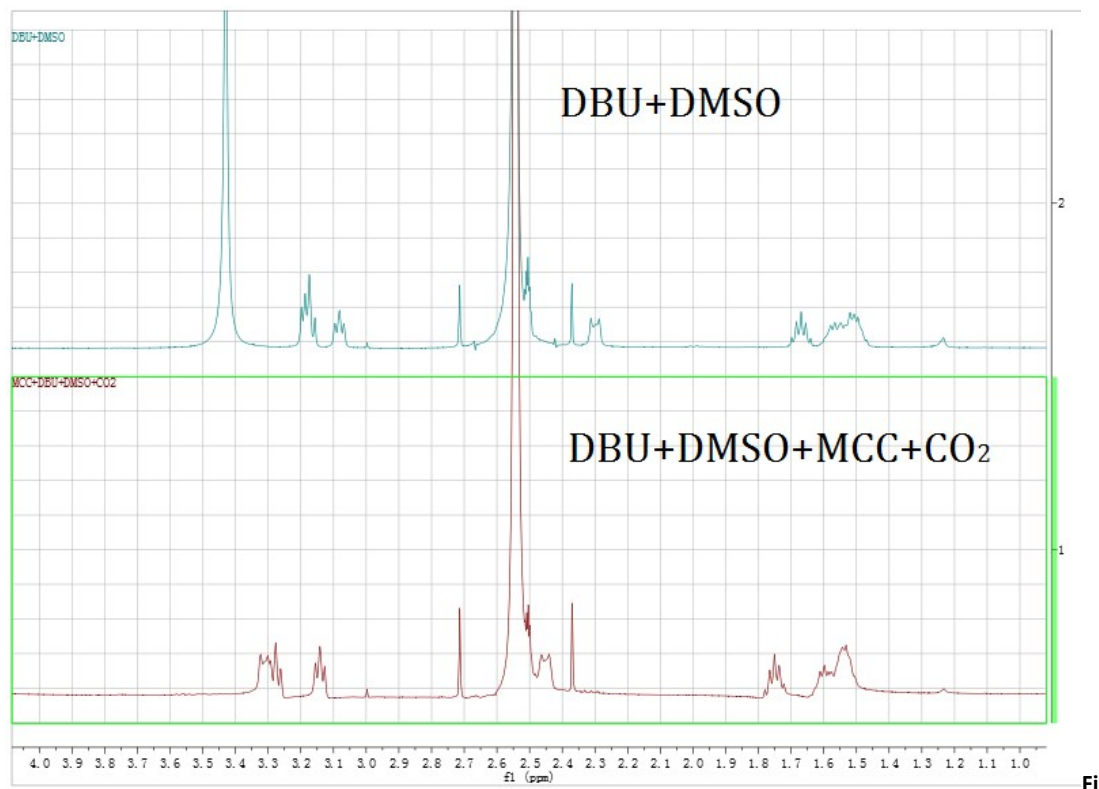


Fig. S4 ATR-FTIR spectra of the formed solutions and their precursors: (a) MCC; (b) DMSO; (c) TMG; (d) DBU; (e) overlap spectra of different concentration MCC dissolving in CO₂-DMSO/TMG solvent system; (f) overlap spectra of different concentration MCC dissolving in CO₂-DMSO/DBU solvent system.

5. Original NMR data

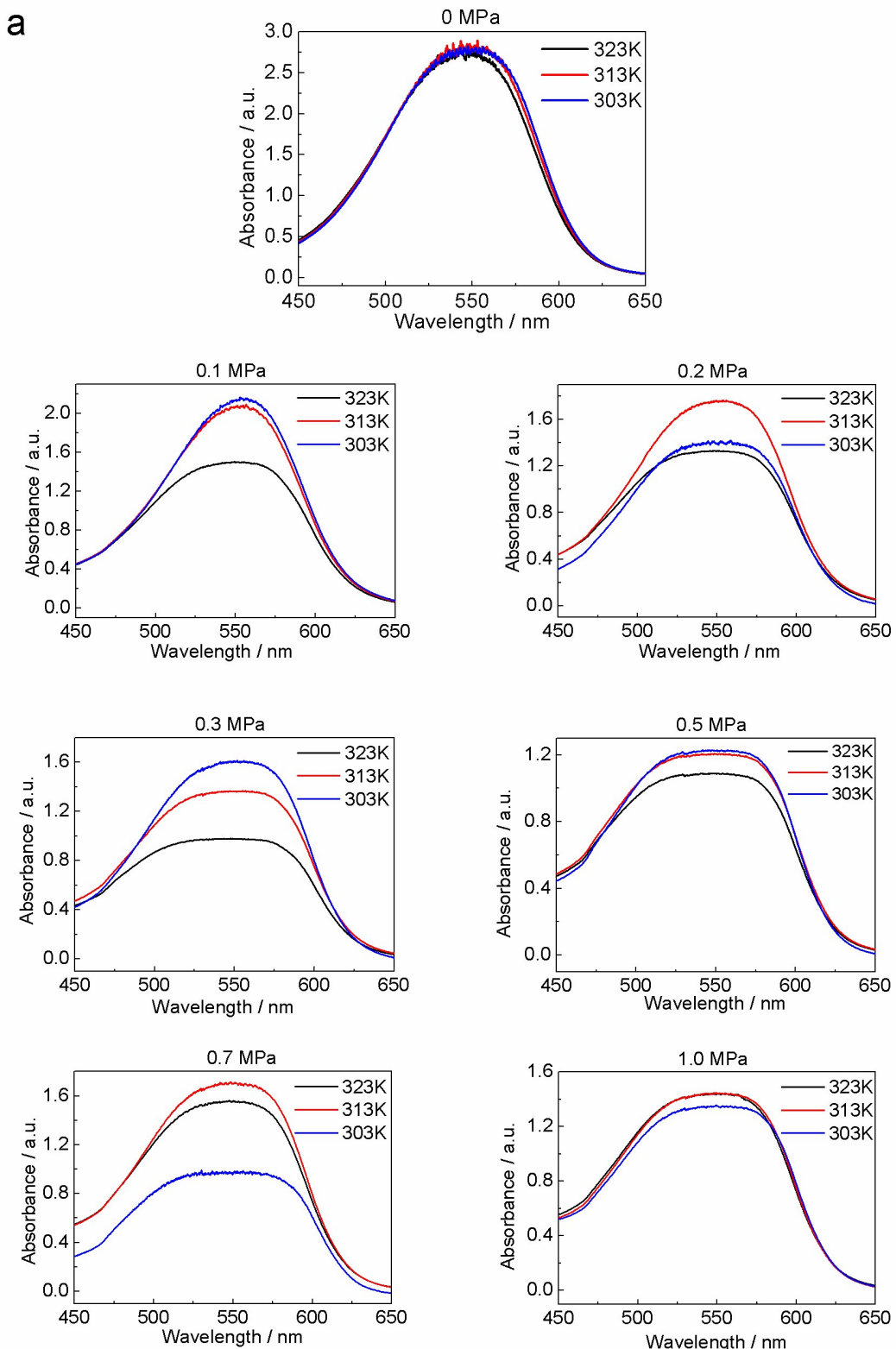


g. S5 Original NMR data of CO₂-DMSO/TMG solvent system with and without MCC



g. S6 Original NMR data of CO₂-DMSO/DBU solvent system with and without MCC

6. Original UV-Vis spectra and instrument photos



b

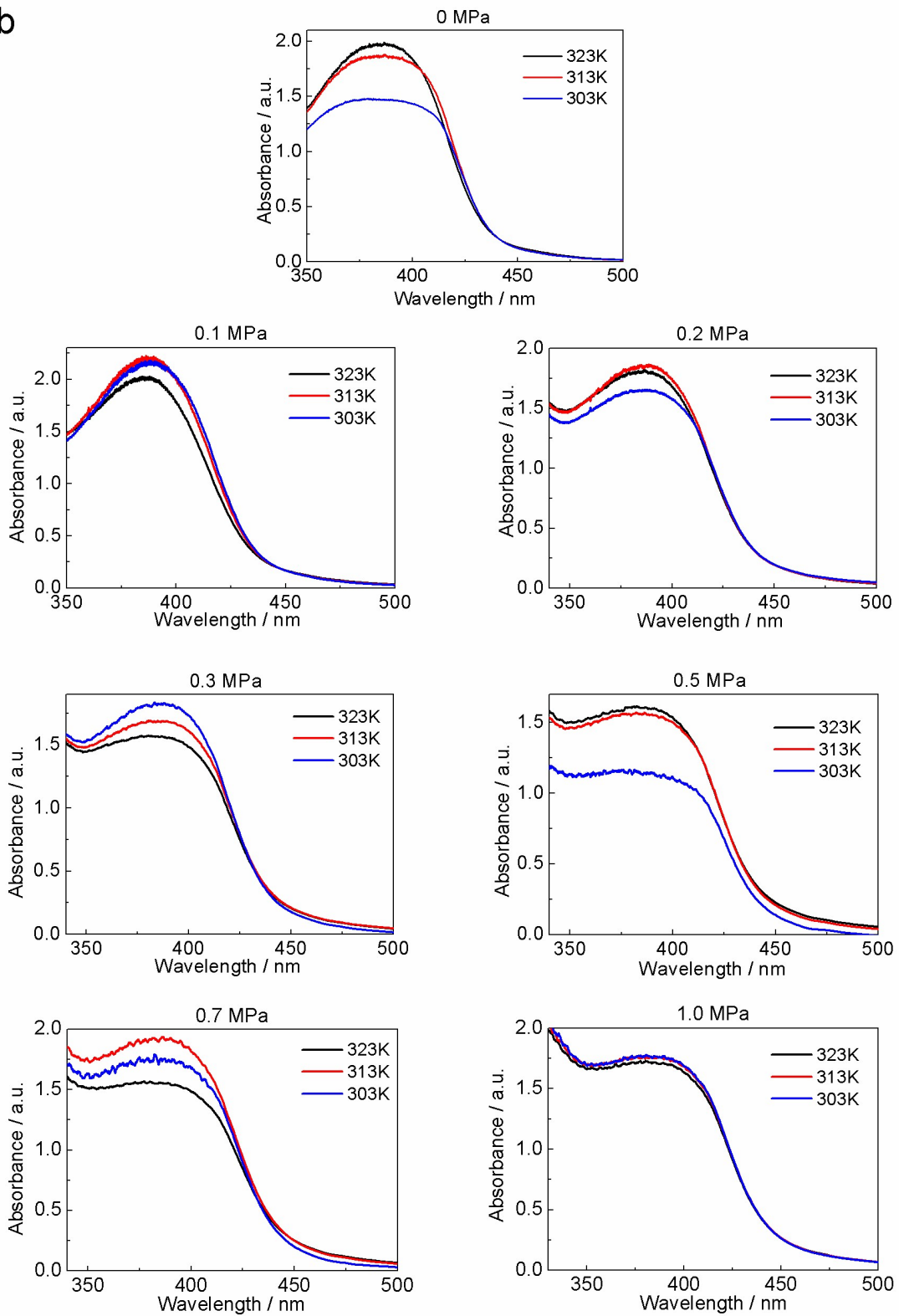


Fig. S7 UV-Vis spectrums of CO_2 -DMSO/DBU solvent system with: (a) Nile red as dye; (b) 4-nitroaniline as dye

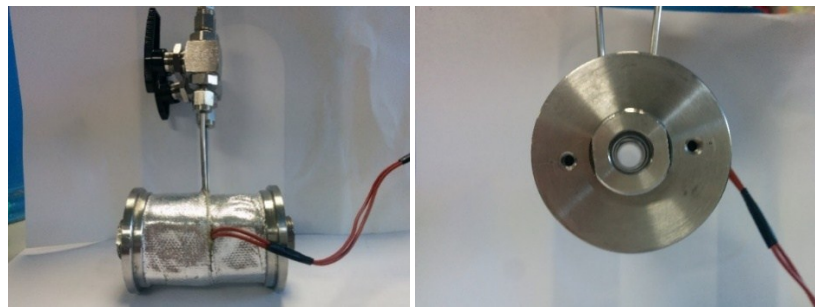


Fig. S8 The photo of high-pressure UV-Vis instrument for measuring the Kamlet-Taft parameters (instrument length: 9 cm; volume, diameter and length of the cuvette are 2.3 ml, 1.2 cm, 2.0 cm, respectively)

7. Electrostatic potential (ESP) results

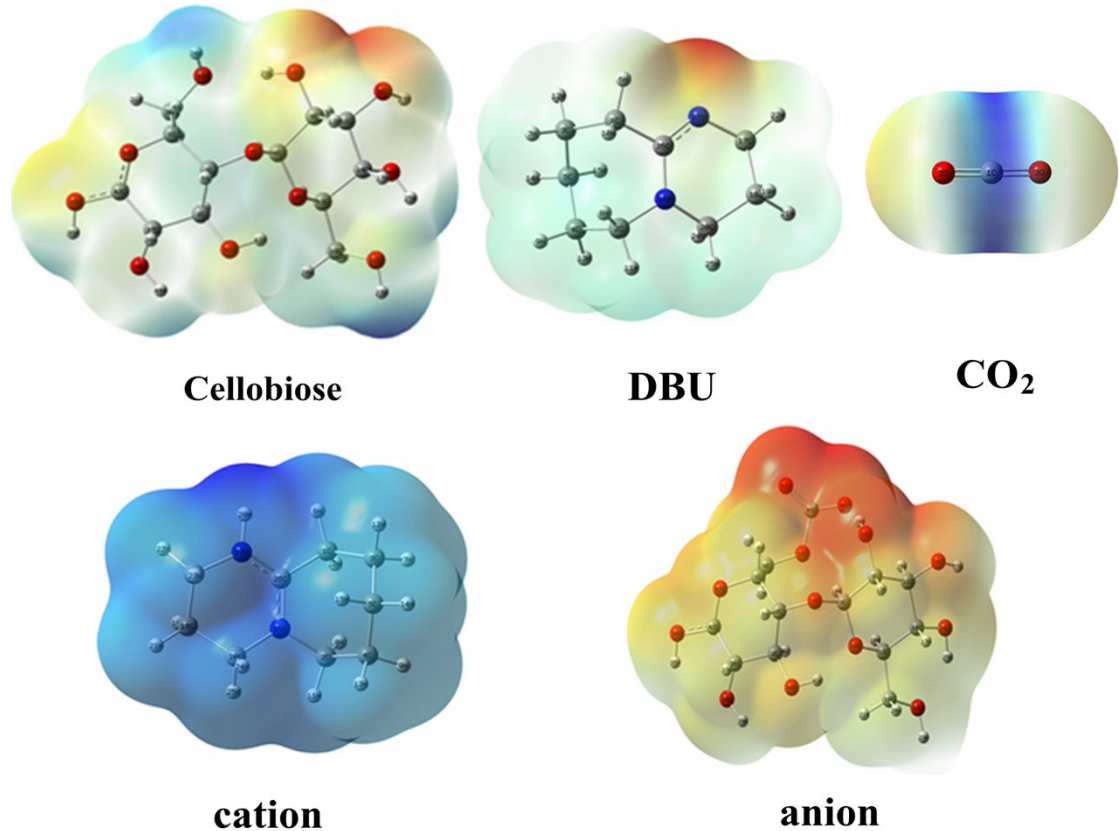


Fig. S9 Electrostatic potential surface of cellobiose, DBU, CO_2 and ions of product computed at the M062X/6-311++G** level. (The regions with positive electrostatic potential and negative electrostatic potential were depicted by blue and red, respectively.)

8. Characterization and analysis of the regenerated cellulose

After precipitation, XRD and TGA measurements were taken for the regenerated cellulose (see in Fig. S10). Fig. S10 (a) shows the XRD diagram of the native and regenerated cellulose. It is obvious that the native cellulose has a better diffraction pattern while regenerated cellulose has a broad peak. The XRD results indicate the cellulose crystalline form changed from I to II, which is consistent with literature results.²⁻⁴ The reason account for the decrystallization of cellulose might be that inter- and intra-molecular hydrogen bonding has been broken partially in the dissolving process. On the other hand, TGA profile shows similar change from cellulose (with only one inflection point) to less stable cellulose (with three inflection point).⁴⁻⁵

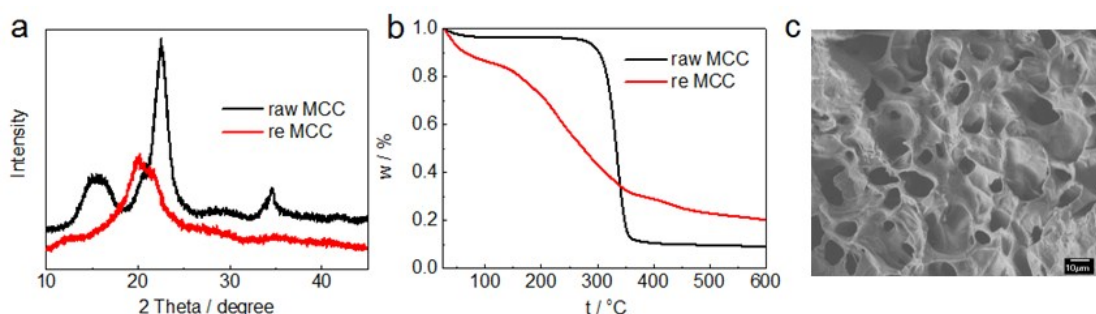


Fig. S10 Differences of the raw cellulose and regenerate cellulose in (a) XRD spectroscopy; (b) TGA diagram; (c) SEM photo of regenerated cellulose after freeze-drying the cellulose solution.

9. Reusability/recyclability of the solvent system

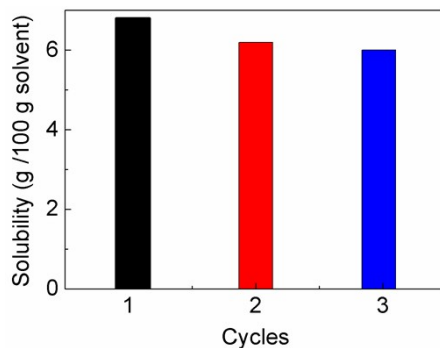


Fig. S11 Cycle times of the DMSO/DBU (5.1 mole percent of DBU) solvent system

REFERENCES

1. Heldebrant, D. J.; Yonker, C. R.; Jessop, P. G.; Phan, L., Organic liquid CO₂ capture agents with high gravimetric CO₂ capacity. *Energy Environ. Sci.* **2008**, *1* (4), 487-493.
2. Zhang, L.; Ruan, D.; Zhou, J., Structure and properties of regenerated cellulose films prepared from cotton linters in NaOH/urea aqueous solution. *Ind. Eng. Chem. Res.* **2001**, *40* (25), 5923-5928.
3. Zhang, L.; Ruan, D.; Gao, S., Dissolution and regeneration of cellulose in NaOH/thiourea aqueous solution. *J.*

Polym. Sci., Part B: Polym. Phys. **2002**, *40* (14), 1521-1529.

4. Sun, X.; Chi, Y.; Mu, T., Studies on staged precipitation of cellulose from an ionic liquid by compressed carbon dioxide. *Green Chem.* **2014**, *16* (5), 2736-2744.
5. Isogai, A., NMR analysis of cellulose dissolved in aqueous NaOH solutions. *Cellulose* **1997**, *4* (2), 99-107.